Journal of the European Ceramic Society 21 (2001) 2863–2872

www.elsevier.com/locate/jeurceramsoc

Dopants for synthesis of stable bimodally porous titania

Jinsoo Kim, Ki Chang Song [1], Sandra Foncillas, Sotiris E. Pratsinis *

Institute of Process Engineering, Swiss Federal Institute of Technology, ETH-Zentrum, CH-8092 Zürich, Switzerland

Received 19 October 2000; received in revised form 12 January 2001; accepted 20 January 2001

Abstract

Bimodally porous titania powders doped with alumina, zirconia, and silica were made by wet precipitation from organometallic precursors (for Al/Ti = 0.05-0.4, and Zr/Ti = Si/Ti = 0.1). Doping retards not only the anatase-to-rutile phase transformation, but also the crystallite growth of titania. So it was used to control the powder phase composition and pore structure at high temperatures. The extent of the retarding effect on pore structure and phase transformation increased with increasing alumina concentration. The effectiveness of these dopants follows the order of: zirconia > silica > alumina. The dopants also reduce the loss of surface area of the calcined powders by decreasing the sintering and phase transformation rates. All powders exhibited bimodal pore size distributions (PSD) with fine intra-particle pores (1–4 nm) and larger inter-particle pores (10–120 nm). However, the intra-particle pores of the pure titania disappeared at 600°C, while the bimodal PSD of doped titania was maintained up to 750°C.

Keywords: Calcining; Crystallite growth; Phase transformations; Porosity; Powders-chemical preparation; TiO_2

1. Introduction

Titania powders can be used as a raw material in electronic and structural ceramics, or as a material for sensors, ceramic membranes,[1–3] adsorbents[4,5] and catalyst supports.[6,7] On a commercial scale, they are typically made in the liquid or gas phase by the sulfate and chloride processes, respectively. The chloride process produces titania particles by oxidation of titanium tetrachloride ($TiCl_4$) vapor in a flame reactor.[8] In the liquid phase, TiO_2 powders are usually prepared by wet precipitation from $TiO(SO_4)$, $Ti(SO_4)_2$, or $TiCl_4$. However, the counter anions of the starting titanium salts may remain in the product and deteriorate the purity of the powders.[9] To avoid counter anion contamination, titanium alkoxides can be used as the starting material for the titania powders. This is justified as alkoxide hydrolysis produces H_2O and eventually CO/CO_2 that are readily removed from the powder by the subsequent calcination that follows sol-gel synthesis.

The titania powders made by wet chemical methods are highly agglomerated[10] with well defined pore structures, while the flame-made powders are less agglomerated giving dense particles. Both powders have large specific surface areas that arise from different structures: well defined pores for powders made by wet chemical methods and very small particles for flame-made powders. The flame-made powders are generally prepared at elevated temperatures and short residence time resulting in rather crystalline rutile powders.[8] In contrast, wet chemical methods use low process (near room) temperature with much longer residence times resulting in amorphous or anatase powders. The wet chemical methods give some unique properties which can not be obtained from flame synthesis. They include precise control of pore structure and dopant concentration.[1,3] Since the porosity depends on the size and structure of primary particles, it can be controlled by manipulating experimental parameters. Brinker et al.[11] extensively investigated pore structure control by managing the packing efficiency, particle aggregation and use of templates during gelation and aging. Barringer and Bowen[12] synthesized monodisperse titania particles by controlled hydrolysis of alcoholic solutions of titanium ethoxide and showed that the average particle size of the titania powders decreased for increased water concentration,

* Corresponding author. Tel.: +41-1-632-3180; fax: +41-1-632-1595.

E-mail address: pratsinis@ivuk.mavt.ethz.ch (S.E. Pratsinis).

[1] On leave from the Department of Chemical Engineering, Konyang University, Nonsan, Chungnam, South Korea.

0955-2219/01/$ - see front matter
PII: S0955-2219(01)00222-9

while it increased slightly with increasing alkoxide concentration. Song and Pratsinis[10] studied the effect of initial water concentration on the characteristics of porous titania powders. They reported that when the initial water concentration was small ($R=[H_2O]/[TTIP]=5$ or 20), the product powder dried at 150°C was amorphous $Ti(OH)_4$ as residual organic components prevented the crystallization to anatase phase. However, when the initial water concentration was large ($R=200$ or 1000), the powders were anatase. The anatase to rutile phase transformation occurring at about 500°C is accompanied by a dramatic change in the grain size and pore structure by sintering.[1,10] Below this temperature, porosity and surface area reduction coming from anatase crystallite growth and sintering is relatively small compared to that attributed to phase transformation.[1] Therefore, for practical applications, it is important to improve thermal stability of titania by retarding the anatase to rutile transformation.

Many researchers studied extensively the retardation of this transformation by doping TiO_2 with a second oxide. This can reduce the sintering rates and nucleation sites (in grain boundary or in bulk) or increase the nucleation activation energy.[3] Kumar et al.[13] studied the effect of alumina on phase and pore structure of titania membranes. They reported that the anatase-to-rutile transformation temperature of the alumina–titania composite membrane (50 wt.% alumina) was 300°C higher than that of pure titania. Yang et al.[14–16] extensively studied the effect of alumina, silica, zirconia, and alumina–silica additives on the titania phase transformation. All these additives showed inhibitory effects on the titania phase transformation, and at the same dopant concentration (dopant/Ti = 0.1), the alumina/silica mixed additive showed the most enhanced retarding effect over other single additives. Vargas et al.[17] investigated the effect of cationic dopants on the temperature of that phase transformation. They chose a large set of metal dopants from different groups of the periodic table to find the relationship between the anatase-to-rutile phase transformation temperature and ionic radii.

Although the above studies addressed the effect of dopants on the phase stability of titania, little is known about the resulting pore structure. The practical applications of the titania at high temperatures depend on, among others, its textural thermal stability. Here, three different dopants (alumina, zirconia and silica) were introduced into titania by co-hydrolysis. This method allows a precise control of dopant concentration and homogeneous mixing of the precursor alkoxide. In addition it avoids an additional drying step required by wet-impregnation method. These dopants were selected since they have been widely used in industry and well investigated in accordance to retard phase transformation. Here the focus is on effect of dopant on the resulting thermal stability of the pore structure. Specifically, the effect of dopant concentration was studied first in synthesis of Al_2O_3-doped TiO_2. Subsequently, Al_2O_3-, ZrO_2-, and SiO_2-doped TiO_2 were studied at a constant dopant concentration to investigate the effect of dopant type and calcination temperature on the phase composition and bimodal pore size distribution of titania.

2. Experimental

Pure and doped titania powders were synthesized by hydrolysis and condensation of titanium tetraisopropoxide (TTIP; $Ti(OC_3H_7)_4$, 97%, Aldrich) and dopants of aluminum tri-sec-butoxide (ATSB; $Al(OC_4H_9)_3$, 97%, Aldrich), zirconium *n*-propoxide (ZNP; $Zr(OC_3H_7)_4$, 70%, Fluka), or tetraethyl orthosilicate (TEOS; $Si(OC_2H_5)_4$, 98%, Aldrich). First, TTIP was dissolved in anhydrous ethyl alcohol at a molar ratio of C_2H_5OH/TTIP = 5. Then, this solution was mixed with a dopant precursor for 1 h to give a constant molar ratio of dopant/Ti = 0.1. Hydrolysis (or co-hydrolysis) was carried out by adding the mixed solution slowly into the distilled water with vigorous stirring for 2 h until a molar ratio of H_2O/TTIP = 20. On adding the water into the mixed solution, white titanium hydroxide precipitates[10] were formed. They were separated from the supernatant liquid with a super-speed centrifuge (Rotina35, Hettich) at 9000 rpm for 10 min. The resulting white cake was dried at 100°C for 24 h, followed by heating at temperatures ranging from 300 to 900°C for 2 h at a heating rate of 10°C/min. When the Al dopant concentration was investigated, the powders were labeled as AT0.05, AT0.1, AT0.2 and AT0.4, respectively, for Al/Ti = 0.05, 0.1, 0.2 and 0.4. The product doped powders were labeled as AT, ZT, and ST for the dopants of alumina, zirconia, and silica, respectively.

An X-ray diffractometer (D5000, Siemens) was used for identification of crystallinity with Ni filtered CuK_α radiation over the range of 2θ from 20 to 60°, with the intensity data for each point being collected at a 4-s interval. XRD was also conducted at $2\theta = 10-60°$ for samples calcined at 900°C in search of Al_2TiO_5 at 15°. The crystallite sizes (D_{hkl}) were calculated by the Scherrer relationship:[18]

$$D_{hkl} = K\lambda/(B_{hkl}\cos\theta) \quad (1)$$

where λ is the wavelength and B_{hkl} is the full width at half maximum, with $K = 0.98$. The weight fraction of rutile in the powder was calculated by:[19]

$$X = 1/[1 + 0.8I_A/I_R] \quad (2)$$

where I_A and I_R are the X-ray integrated intensities of the (101) reflection of anatase and the (110) reflection of rutile.

The specific surface area, pore volume and pore size distribution of the pure and doped titania powders were obtained by N_2 adsorption/desorption at 77 K in a Micromeritics ASAP 2010. All powders were degassed at 100°C prior to measurement. The specific surface area was determined by the multipoint BET method using the adsorption data in the relative pressure (P/P_0) range of 0.05–0.25. The pore size distribution data were calculated by the ASAP 2010 software from the N_2 desorption isotherms. The Barrett, Joyner, and Halender (BJH) method[20] with cylindrical pore size calculated from the Kelvin equation was used in the data processing. The results obtained by the preparation of pure and doped titania powders and their characterization by adsorption porosimetry were reproduced at least twice within an error of 15%.

3. Results and discussion

3.1. Effect of Al_2O_3 dopant concentration

The effect of dopant on pore/phase structure was investigated by doping TiO_2 with different Al_2O_3 concentrations (5–40 mol%). All alumina doped titania powders are amorphous after calcining at 300°C. The anatase peaks start to appear at 450°C for titania powder containing 5 mol% alumina (AT0.05), and at 600°C for titania powders containing 10 and 20 mol% alumina (AT0.1 and AT0.2, respectively). However, titania powder containing 40 mol% alumina (AT0.4) begins to show anatase peaks after calcining at 750°C. On the other hand, all alumina doped titania powders showed only anatase phase till 750°C, and the anatase-to-rutile phase transformation started to occur after calcining at 900°C. Also, the XRD data show that all alumina doped titania powders show α-alumina peaks at 900°C. The α-alumina peaks become more noticeable with increasing alumina dopant concentration as shown in Fig. 1. However, aluminum titanate (Al_2TiO_5) was not found in this experiment, even at the high alumina dopant concentration (AT0.4). This phase composition evolution is in agreement with Yang et al.[14] In contrast, it disagrees with Kumar et al.[13] who prepared alumina doped titania membranes with peptization.

The anatase crystallite sizes, calculated from Eq. (1), are given in Fig. 2 as a function of alumina dopant concentration. At any calcination temperature the size of anatase decreased with increasing alumina concentration. At 600°C the crystallite sizes of AT0.05, AT0.1 and AT0.2 powders are almost the same. With increasing calcination temperature to 750°C, the crystallite sizes differ showing the inhibiting effect of alumina on crystallite growth. However, AT0.05 powder shows a sharp size increase of crystallite size from 10.8 nm at 600°C to 38.7 nm at 750°C. This suggests that doping less alumina (<5 mol%) is not effective in retarding anatase crystallite growth especially at high temperatures.

Fig. 3 shows the variation in specific surface area (SSA) for alumina doped titania as a function of dopant concentration. Titanias produced in the absence of dopant have the lowest SSA at all temperatures. The SSA decreases with increasing calcination temperature by phase transformation and sintering (crystallite growth). At a constant dopant concentration, there is a certain calcination temperature which results in a sharp decrease in the SSA (Fig. 3). For pure titania and AT0.05 powders, this occurs from 300 to 450°C, while for the other powders, from 450 to 600°C. As a result of this and the above XRD data, detailed investigations are carried out with Al_2O_3-doped TiO_2 of 10%. This drastic decrease in the SSA is accompanied by the transformation from

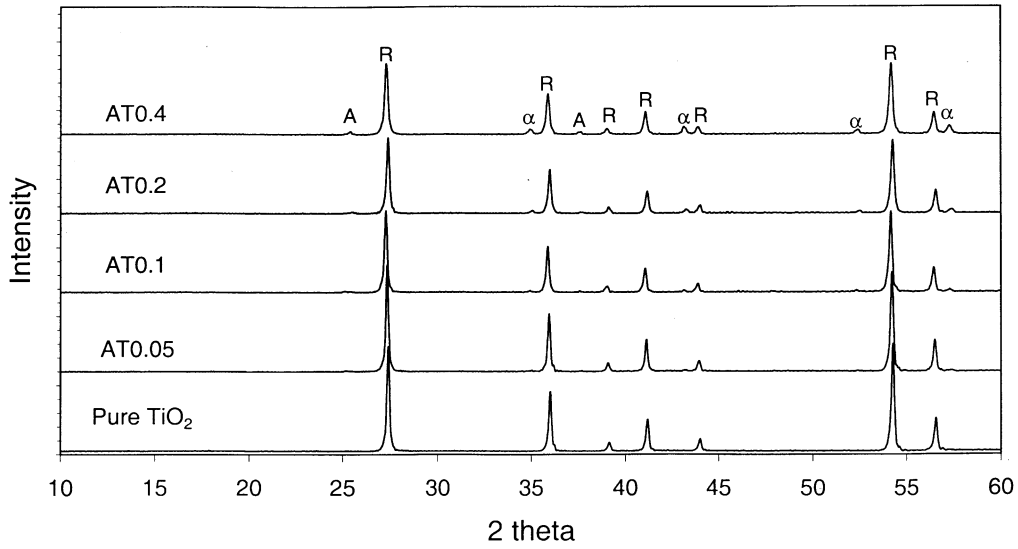

Fig. 1. XRD patterns of the Al_2O_3-doped TiO_2 after being calcined at 900°C for 2 h (A: anatase, R: rutile, α: α-Al_2O_3).

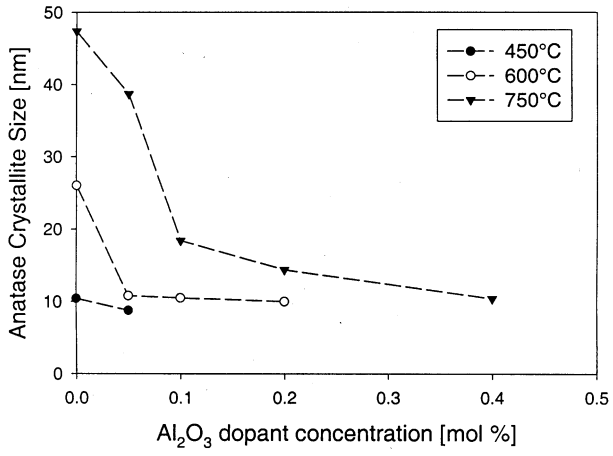

Fig. 2. Anatase crystallite sizes of the Al_2O_3-doped TiO_2 as a function of dopant concentration.

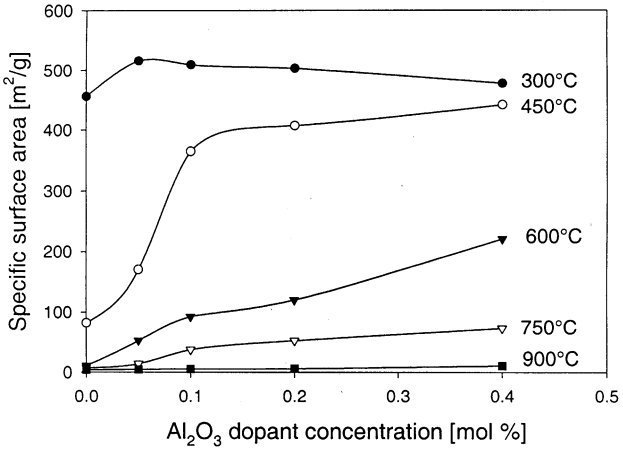

Fig. 3. Specific surface areas of the Al_2O_3-doped TiO_2 as a function of dopant concentration.

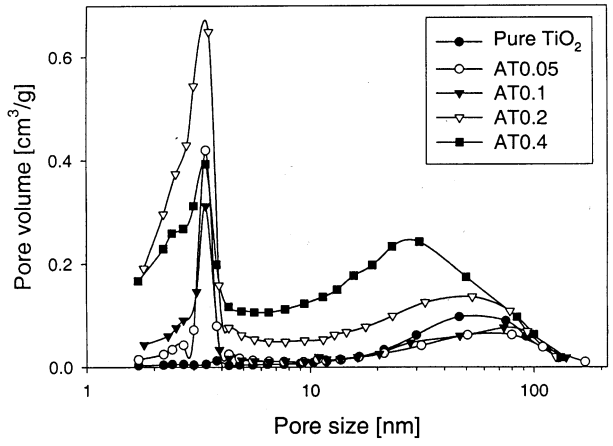

Fig. 4. Pore size distributions of the Al_2O_3-doped TiO_2 as a function of dopant concentration after calcined at 600°C for 2 h.

amorphous to anatase. Generally, the phase transformation results in a dramatic pore structure change, comparing to the sintering (crystallite growth).

Fig. 4 shows the pore size distributions of Al-doped titania calcined at 600°C as a function of Al_2O_3 dopant concentration. All the alumina doped titanias show bimodal pore size distributions of smaller intra-particle pores (1–4 nm in diameter) and larger inter-particle pores (10–120 nm). However, both inter-particle pores and intra-particle pores are broader with increasing Al_2O_3 dopant concentration. It is interesting to note that alumina doped titania membranes showed the opposite results.[1,13] Kumar et al.[1,13] reported that the pore size distribution became sharper with increasing alumina concentration and the maximum pore volume shifted right indicating pore growth with decreasing alumina concentration.

Although Kumar et al.[13] studied the effect of alumina dopant concentration on titania membrane textural stability, it is not easy to directly compare these with the present results because membranes were created on substrates while the powders here were not. For example, the AT0.4 powder (51 wt.%) and titania-alumina composite membrane (50 wt.%) could be compared after heat treated at 900°C, since they have similar alumina concentrations. Although they showed the similar crystallinity, the membrane maintained higher porosity (23%) than the AT0.4 powder (12%). Considering the holding time at that sintering temperature (2 h for powder and 8 h for membrane), it is evident that the membrane has more stable pore structure. Membranes, however, were prepared on rigid supports that can interfere with the creation of the porosity and phase transformation as seeds always affect the characteristics of product powders.[1]

From the above results, it is clear that the presence of alumina in titania powder retarded the crystallite growth and phase transformation and thereby improved the textural properties at high temperatures. The extent of this retarding effect increased with increasing alumina content. As shown in Fig. 1, however, doping less alumina (5 mol%) was not so effective in retarding crystallite size growth and phase transformation rate in agreement with Yang et al.[14] Therefore, we fixed the alumina dopant concentration at 10% and compared with other dopants at the same dopant concentrations.

3.2. Phase composition

Fig. 5a–d shows the XRD patterns of pure and doped titania powders (at dopant/Ti = 0.1) calcined at different temperatures. As shown in Fig. 5a, the pure titania dried at 100°C is amorphous[10] for $R = 20$. Heating that powder not only consolidated it but also facilitated the phase transformation from amorphous to metastable anatase and then to stable rutile phase.[10] The XRD patterns of doped titania powders show a similar trend in Fig. 5b–d, although the doping increased the temperature of phase transformation. It should be noted

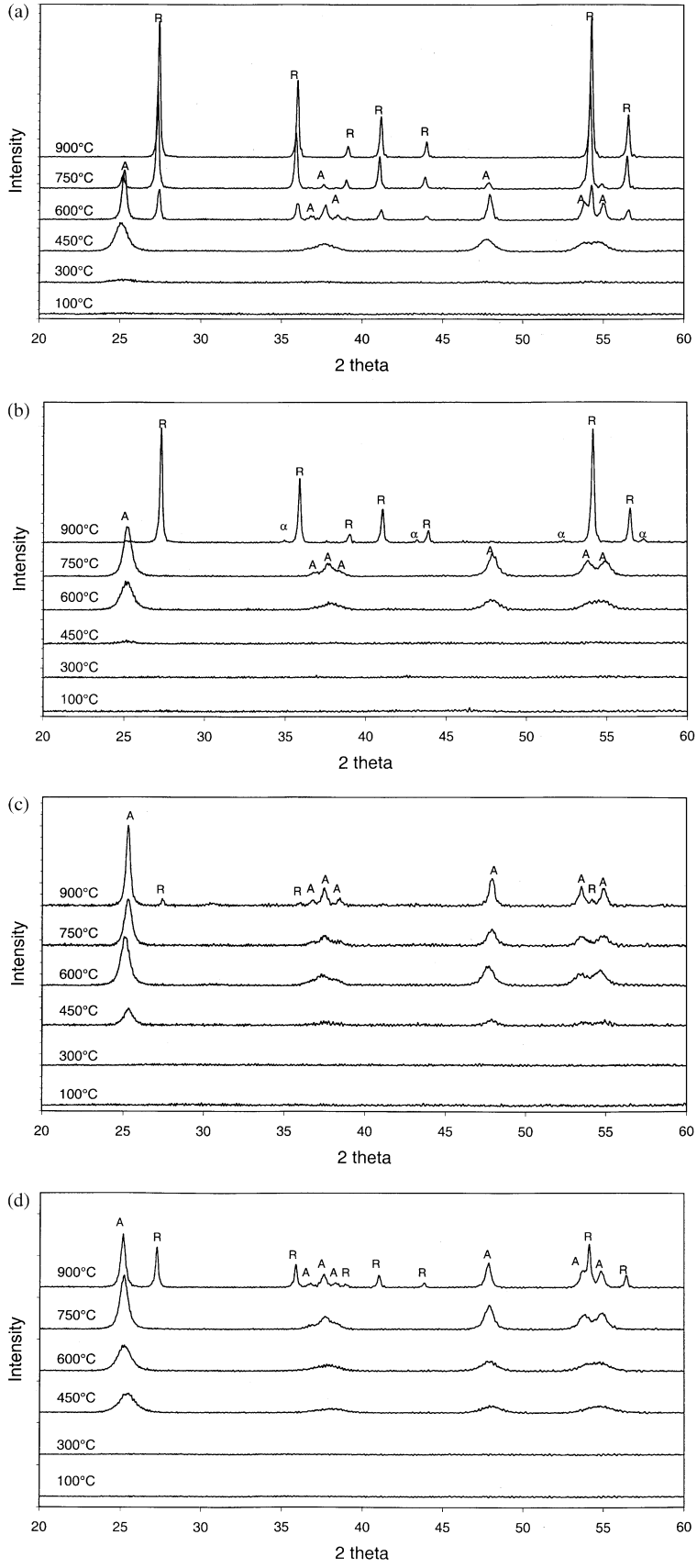

Fig. 5. XRD patterns of titania powder: (a) pure and doped with (b) alumina (AT), (c) zirconia (ZT), and (d) silica (ST) as a function of calcination temperature (A: anatase, R: rutile, α: α-Al_2O_3).

that there is no real phase transformation temperature for a metastable-to-stable phase transformation, as in the case of a reversible transformation at equilibrium (one stable phase to another stable phase). In this case, the phase transformation is dictated by kinetics, which are determined by the lattice structure of each phase, grain size, and number of nucleation sites.[3]

As shown in Fig. 5, all pure and doped titania powders are amorphous till 300°C. The anatase peaks start to appear at 450°C for pure titania, zirconia-doped (ZT) and silica-doped (ST) powders while the alumina doped titania powder (AT) begins to show anatase peaks much later at 600°C. The anatase-to-rutile transformation starts at 600°C for pure titania powder while all doped titania powders remain anatase up to 750°C, while the rutile phase appears at 900°C. Although the phase transformation temperatures (from amorphous to anatase and from anatase to rutile) depend on the dopant, it is apparent that alumina, zirconia and silica dopants retard the first phase transformation from amorphous to tetragonal titania consistent with prior research.[13–17]

In Fig. 5c and d, the XRD data for Zr- and Si-doped powders show that no other phases than tetragonal titania are detected by XRD. This indicates that no ZrO_2 or SiO_2 crystals with XRD detectable size were formed in these powders. On the other hand, AT powder shown in Fig. 4b begins to show α-alumina peaks at 900°C, which is much lower than that reported for pure alumina (about 1230°C).[21] Slepetys and Vaughan[22] reported that the maximum Al_2O_3 solubility in rutile phase was about 2 mol% at 1699 K. Therefore, when the temperature was increased to a level which allows the anatase to rutile transformation to occur, the α-Al_2O_3 was formed from the exsolution of the as-formed anatase solid solution due to the limited Al_2O_3 solubility. These α-Al_2O_3 peaks that appeared at lower temperature were also observed by Yang and Ferreira[15] who reported that the as-formed α-Al_2O_3 reacted with rutile to form aluminum titanate (Al_2TiO_5) when the calcination temperature was further increased to 1225°C. The aluminum titanate was detected at $2\theta = 15°$. However, aluminum titanate was not found in this experiment, as a lower calcination temperature (900°C) was used here. The XRD results, especially for anatase, suggest that the dopants are either present in a form of two-dimensional layer or are incorporated into the lattice structure of titania. However, identification of the exact state of the dopants in nanostructured powders is rather difficult. Akhtar et al.,[23] however, had showed by XPS and XRD that most of the Al-dopant is on the surface of TiO_2 particles made in a hot wall aerosol reactor by $TiCl_4$ oxidation. They found aluminum titanate at 1700 K.

Fig. 6 shows the anatase crystallite size as a function of calcination temperature for pure and doped titania powders. The crystallite size of pure titania increases

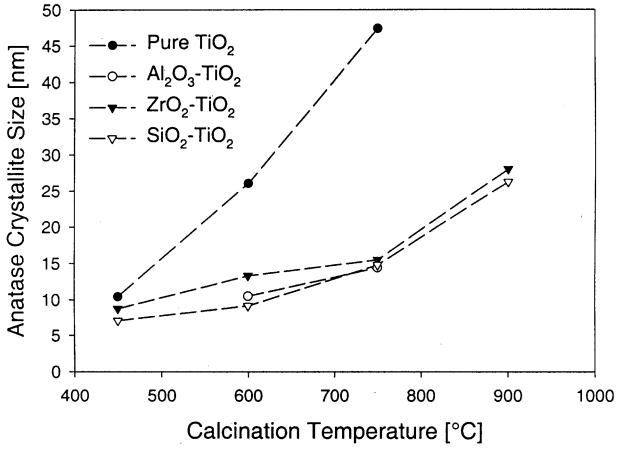

Fig. 6. Anatase crystallite sizes of the titania powders with various dopants as a function of calcination temperature.

rapidly with increasing temperature. On the other hand, the doped titania powders show a rather slow increase in crystallite sizes up to 750°C. At 750°C, the crystallite size of pure titania is 47.4 nm, while the crystallite sizes of TiO_2 doped with Al_2O_3, ZrO_2 and SiO_2 are only 14.4, 15.0 and 14.7 nm, respectively. However, all doped titanias show higher growth of crystallites above 750°C by phase transformation and sintering. Although the rutile sizes are not presented here, the stable rutile phase has a larger grain size (> 50 nm) than that of the metastable anatase phase (7–30 nm) as indicated by sharper peaks in XRD patterns (Fig. 5). In general, both anatase and rutile grain sizes of doped titania are smaller than those of pure titania processed at the same temperature. Hence, the presence of alumina, zirconia, and silica dopants in titania retards the crystallite growth of titania and also the anatase-to-rutile phase transformation. From the XRD patterns at 900°C, the rutile weight fractions are calculated as 98.7, 10.2 and 48.7%, respectively, for AT, ZT and ST powders. This variation in the extent of transformation suggests that the effectiveness of the retarding effect on the anatase to rutile phase transformation by the dopants is: zirconia > silica > alumina consistent with the data of Yang et al.[15,16]

3.3. Specific surface area and porosity

Fig. 7 shows the specific surface area (SSA) of the pure and doped titania powders (dopant/Ti = 0.1) as a function of calcination temperature. All powders show a decrease of the SSA with increasing calcination temperature by phase transformation and sintering (crystallite growth). The specific surface areas of all powders are similar at 300°C, but differ at 450°C. This can be explained by Fig. 5, where the pure, ZrO_2- and SiO_2-doped titania powders start to show anatase peaks at 450°C while the Al_2O_3-doped titania powder is still amorphous. This crystallization is usually accompanied

by a steep decrease of the SSA[10] as shown in Fig. 7. After calcined at 600°C for 2 h, the doped titania powders have SSAs of 88–103 m^2/g with anatase phase only, while the pure titania powder has a SSA of about 10 m^2/g containing both anatase and rutile phases. With increasing the calcination temperature over 750°C, the difference in SSA between pure and doped titania powders decreases, since all powders become rutile.

With increasing calcination temperature, the pore volume of pure and doped TiO_2 decreases continuously (Fig. 8). The ZrO_2-doped titania shows the highest pore volume indicating that it has the highest porosity up to 750°C. It is interesting to see that the pore volume of Al_2O_3-doped TiO_2 decreases relatively slowly at 450°C in agreement with Kumar et al.[13] This may be attributed to the negative volume change of the alumina phase in the powder.

Fig. 9 shows the isotherms of pure and doped titania powders calcined at 600°C. All doped titania powders show isotherms of type IV (BDDT classification) which exhibit hysteresis loops mostly of type H3.[20] This indicates that the powders contain mesopores (2–50 nm) with narrow slit-like shapes. Also, the isotherms show two hysteresis loops, showing bimodal pore size distributions in the mesoporous region ($d_p > 2$ nm), as shown in Fig. 10 as calculated from Fig. 9. On the other hand, the isotherm of pure titania is of type V with one hysteresis loop of type H3, indicating a monomodal pore size distribution[10] at this temperature arising from the collapse of the intra-particle pores at 600°C. On the contrary, all doped titania powders calcined at 600°C show bimodal pore size distributions consisting of smaller fine (2–10 nm) intra-particle pores and larger (10–120 nm) inter-particle pores. Kumar et al.[24] also reported a bimodal pore size distribution made from fine intra-aggregated pores (represented by the hysteresis loop in the lower P/P_0 range) and larger inter-aggregated pores (hysteresis loop in the higher P/P_0 range) arising from hard aggregates. A typical bimodal microstructure was presented in Fig. 11. The pores

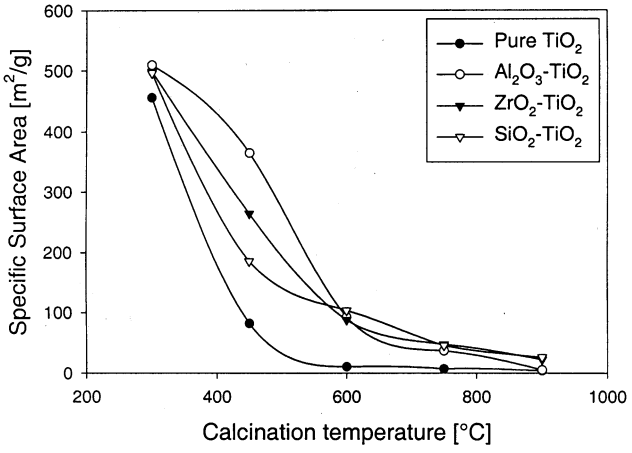

Fig. 7. Specific surface areas of the titania powders with various dopants as a function of calcination temperature.

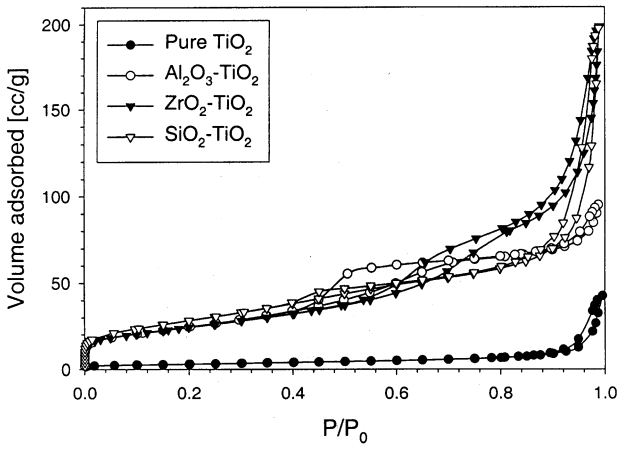

Fig. 9. Isotherms of the titania powders with various dopants after being calcined at 600°C for 2 h.

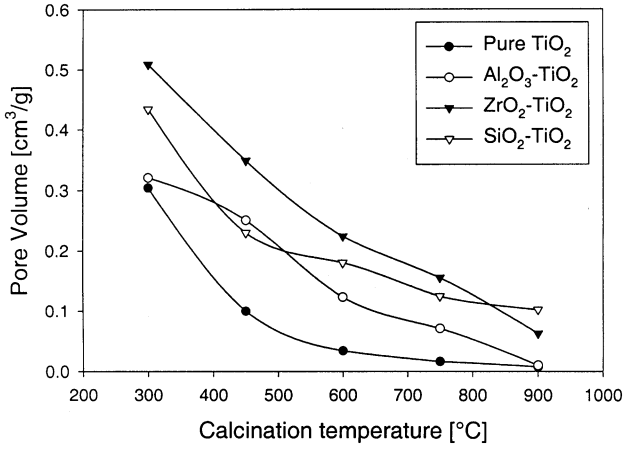

Fig. 8. Pore volumes of the titania powders with various dopants as a function of calcination temperature.

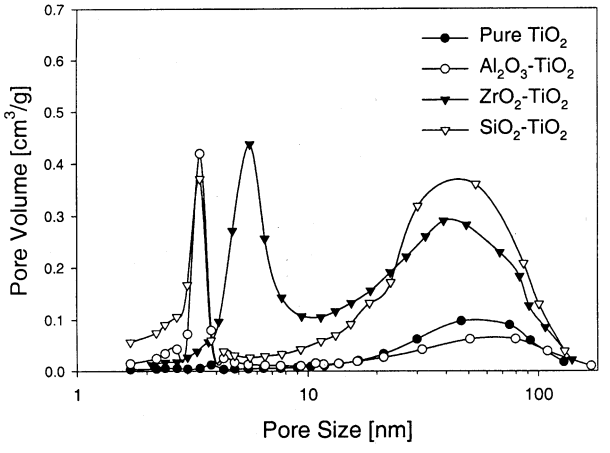

Fig. 10. Pore size distributions of the titania powders with various dopants after being calcined at 600°C for 2 h.

within the hard aggregates give the intra-particle pores, while the voids between these aggregates give the inter-particle pores.[25] It is interesting to observe that different dopants show different pore size distributions. From Fig. 10, both Al_2O_3- and SiO_2-doped powders have the same average pore size of intra-particle pores (3.4 nm), while the ZrO_2-doped titania powder has a larger average intra-particle pore size (5.6 nm). On the other hand, Al_2O_3-doped titania powder has much smaller inter-particle pore volume comparing to the other doped titania powders. The isotherms were of type IV with two hysteresis loops for pure and doped titania powders at lower calcination temperatures (<600°C), indicating bimodal pore size distributions also. Fig. 12a–d show the pore size distributions of pure and doped titania powders as a function of calcination temperature. With increasing calcination temperature above 600°C, the average pore size of the intra-particle pores shifts to the right indicating the growth of pores, while the inter-particle pores stay more or less at the same size range just showing the decrease of pore volume. Also, it is interesting to note that the inter-particle pore volumes of ZT and ST powders are much bigger than those of pure titania and AT powders. This indicates that ZT and ST powders consist of more hard aggregates than the AT ones, since the inter-particle pores arise from the voids between aggregates. After calcining at 600°C, the intra-particle pores of the pure titania powder disappeared completely as shown in Fig. 12a, while the other doped titania powders maintained the bimodal pore size distributions up to 750°C in Fig. 12b–d. Both pure and doped titania exhibit monomodal pore size distribution due to the complete collapse of the intra-particle pores at 900°C as their SSA has been reduced to about 10 m^2/g for all of them (Fig. 7).

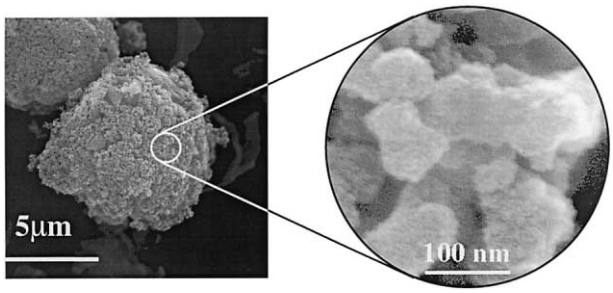

Fig. 11. SEM of spray dried titania powders with bimodal porosity.[25]

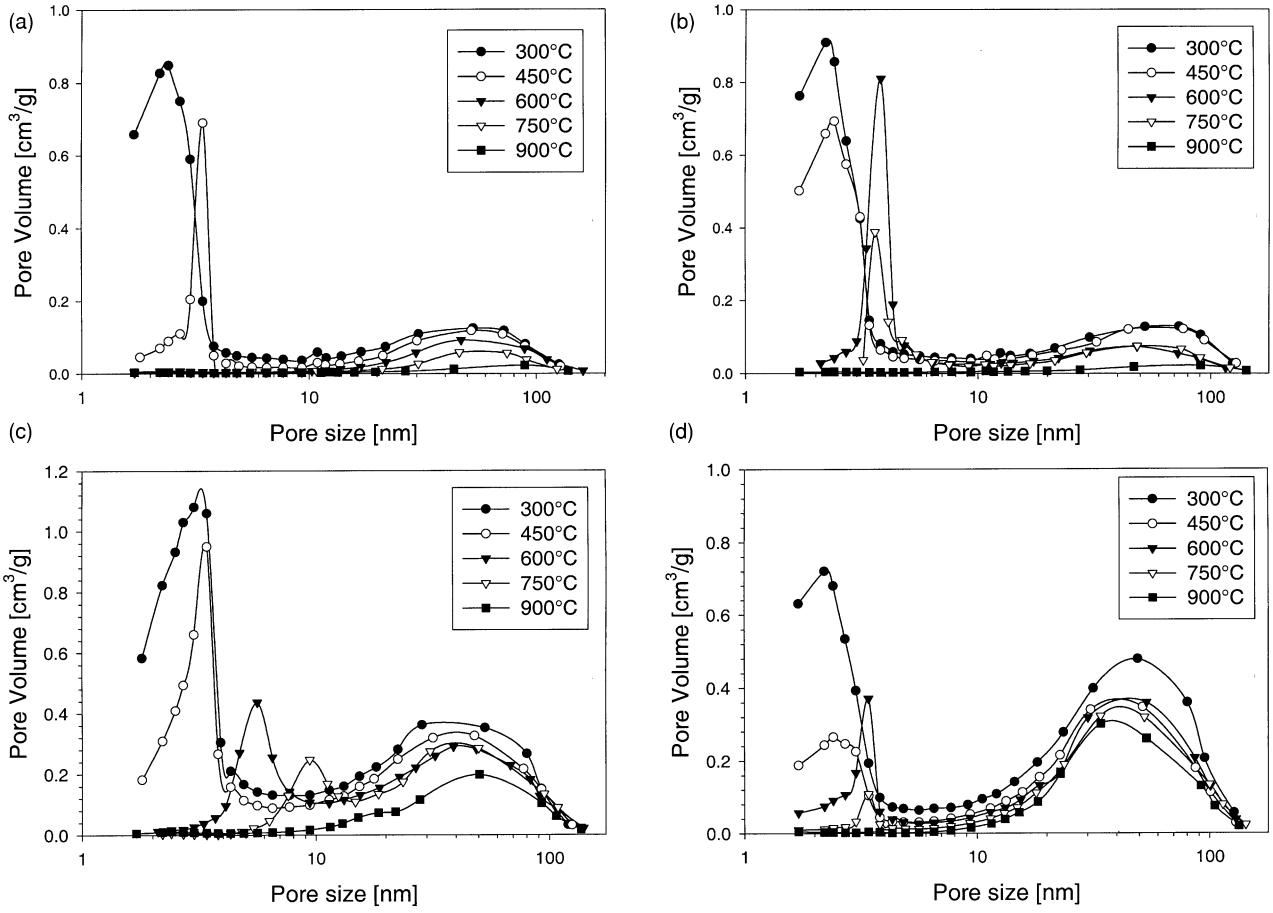

Fig. 12. Evolution of pore size distributions with calcination temperature: (a) pure titania; (b) AT; (c) ZT; (d) ST powders.

Another interesting result from Fig. 12 is that the main cause of the disappearance of most intra-particle pores at different temperatures could be attributed to grain growth from the phase transformation of anatase to rutile, as confirmed in Figs. 5 and 6. Kumar et al.[1] observed the microstructures of titania membranes calcined at various temperatures by high resolution scanning electron micrograph. They observed that the powders before the anatase to rutile transformation contain small anatase crystallites, but the powders after transformation have smaller anatase crystallites and bigger densified rutile regions. It is thought that smaller anatase crystallites grow into bigger rutile crystallites through the transformation, leading to the disappearance of the voids between anatase crystallites which results in the collapse of intra-particle pores in the bimodal pore size distributions.

Finally, it should be noted that doping a second oxide cannot completely retard the structure change of the powders at elevated temperatures. But the results presented above have clearly demonstrated that doping alumina, zirconia and silica retards the crystallite growth and phase transformation up to 750°C. This resulted in a subsequent stabilization of the porous texture of titania. The improvement on the stability of the pore structure is more significant if one considers the time scale, since the change of the pore structure or composition due to sintering or phase transformation depends exponentially on the temperature but linearly on time.[26,27]

4. Conclusions

Alumina, zirconia and silica doped titania powders were prepared by the co-hydrolysis and condensation of their precursors. All doped titania powders retarded the anatase-to-rutile phase transformation and showed a significantly improved textural stability compared to the pure titania powder. When different alumina dopant concentration was applied, the extent of the retarding effect on pore structure and phase transformation increased with increasing alumina concentration. However, doping less alumina (<5 mol%) was not effective in improving pore structures especially at higher temperatures. The significance of the retarding effect on the anatase to rutile phase transformation by the dopants is: zirconia > silica > alumina. After heat treatment at 600°C for 2 h, the doped titania has a specific surface area of 88–193 m^2/g in anatase phase, while pure titania has a specific surface area of about 10 m^2/g in anatase and rutile phases. All as-synthesized powders showed bimodal pore size distributions with fine intra-particle pores and larger inter-particle pores. However, the intra-particle pores of pure titania powder disappeared at 600°C, while the doped titania powders maintained bimodal pore size distributions up to 750°C.

Acknowledgements

This research was sponsored by SNF (Swiss National Science Foundation), KTI (Top Nano 21) and ETH Zürich.

References

1. Kumar, K.-N. P., Keizer, K. and Burggraaf, A. J., Textural evolution and phase transformation in titania membranes. *J. Mater. Chem.*, 1993, **3**, 1141–1149.
2. Wu, L. Q., Huang, P., Xu, N. P. and Shi, J., Effects of sol properties and calcination on the performance of titania tubular membranes. *J. Membr. Sci.*, 2000, **173**, 263–273.
3. Chang, C. H., Gopalan, R. and Lin, Y. S., A comparative study on thermal and hydrothermal stability of alumina, titania and zirconia membranes. *J. Membr. Sci.*, 1994, **91**, 27–45.
4. Tani, K. and Suzuki, Y., Syntheses of spherical silica and titania from alkoxides on a laboratory-scale. *Chromatographia*, 1994, **38**, 291–294.
5. Tani, K. and Suzuki, Y., Investigation of the ion-exchange behaviour of titania: application as a packing material for ion chromatography. *Chromatographia*, 1997, **46**, 623–627.
6. Nair, P., Mizukami, F., Okubo, T., Nair, J., Keizer, K. and Burggraaf, A. J., High-temperature catalyst supports and ceramics membranes: metastability and particle packing. *AIChE J.*, 1997, **43**, 2710–2714.
7. Matsuda, S. and Kato, A., Titania oxide based catalysts: a review. *Appl. Catal.*, 1983, **8**, 149–165.
8. Pratsinis, S. E., Flame aerosol synthesis of ceramic powders. *Prog. Energy Combust. Sci.*, 1998, **24**, 197–219.
9. Kominami, H., Takada, Y., Yamagiwa, H., Kera, Y., Inoue, M. and Inui, T., Synthesis of thermally stable nanocrystalline anatase by high-temperature hydrolysis of titanium alkoxide with water dissolved in organic solvent from gas phase. *J. Mater. Sci. Lett.*, 1996, **15**, 197–200.
10. Song, K. C. and Pratsinis, S. E., Synthesis of bimodally porous titania powders by hydrolysis of titanium tetraisopropoxide. *J. Mater. Res.*, 2000, **15**, 2322–2329.
11. Brinker, C. J., Sehgal, R., Hietala, S. L., Deshpande, R., Smith, D. M., Loy, D. and Ashley, C. S., Sol-gel strategies for controlled porosity inorganic materials. *J. Memb. Sci.*, 1994, **94**, 85–102.
12. Barringer, E. A. and Bowen, H. K., Formation, packing and sintering of monodisperse TiO_2 powders. *J. Am. Ceram. Soc.*, 1982, **65**, C199–C201.
13. Kumar, K.-N.P., Keizer, K. and Burggraaf, A. J., Textural stability of titania-alumina composite membranes. *J. Mater. Chem.*, 1993, **3**, 917–922.
14. Yang, J., Huang, Y. X. and Ferreira, J. M. F., Inhibitory effect of alumina additive on the titania phase transformation of a sol-gel-derived powder. *J. Mater. Sci. Lett.*, 1997, **16**, 1933–1935.
15. Yang, J. and Ferreira, J. M. F., Inhibitory effect of the Al_2O_3-SiO_2 mixed additives on the anatase-rutile phase transformation. *Mater. Lett.*, 1998, **36**, 320–324.
16. Yang, J. and Ferreira, J. M. F., On the titania phase transition by zirconia additive in a sol-gel derived powder. *Mater. Res. Bull.*, 1998, **33**, 389–394.
17. Vargas, S., Arroyo, R., Haro, E. and Rodriguez, R., Effects of cationic dopants on the phase transition temperature of titania prepared by the sol-gel method. *J. Mater. Res.*, 1999, **14**, 3932–3937.
18. Cullity, B. D., *Elements of X-ray Diffraction*. Reading, MA, 1987.
19. Spurr, R. A. and Myers, H., Quantitative analysis of anatase-rutile mixtures with an X-ray diffractometer. *Anal. Chem.*, 1957, **29**, 760.

20. Sing, K. S. W., Everett, D. H., Haul, R. A. W., Moscou, L., Pierotti, R. A., Rouquerol, J. and Siemieniewska, T., Reporting physisorption data for gas/solid systems-with special reference to the determination of surface area and porosity. *Pure Appl. Chem.*, 1985, **57**, 603–619.
21. Mcardle, J. L. and Messing, G. L., Seeding with gamma-alumina for transformation and microstructure control in boehmite-derived alpha-alumina. *J. Am. Ceram. Soc.*, 1986, **69**, C58–C101.
22. Slepetys, R. A. and Vaughan, P. A., Solid solution of aluminum oxide in rutile titanium dioxide. *J. Phys. Chem.*, 1969, **73**, 2157–2162.
23. Akhtar, M. K., Mastrangelo, S. V. R. and Pratsinis, S. E., Vapor phase synthesis of Al-doped titania powders. *J. Mater. Res.*, 1994, **9**, 1241–1249.
24. Kumar, K.-N.P., Kumar, J. and Keizer, K., Effect of peptization on densification and phase-transformation behavior of sol-gel derived nanostructured titania. *J. Am. Ceram. Soc.*, 1994, **77**, 1396–1400.
25. Kim, J., Song, K. C., Wilhelm, O. and Pratsinis, S. E., Sol-gel synthesis and spray granulation of porous titania powder. *Chem. Ing. Technol.*, submitted.
26. German, R.M., Simulation of diffusion controlled sphere-sphere sintering. In *Sintering—New Development*, ed. M. M. Ristic, Elsevier, Amsterdam, 1977.
27. Brinker, C. J. and Scherer, G. W., *Sol-Gel Science: the Physics and Chemistry of Sol-Gel Processing*. Academic Press, Boston, 1990.